DOI: 10.1007/s11099-017-0715-2 PHOTOSYNTHETICA 56 (2): 652-659, 2018

Investigating role of Triton X-100 in ameliorating deleterious effects of anthracene in wheat plants

C. SHARMA, S. MATHUR, R.S. TOMAR, and A. JAJOO+

School of Life Science, Devi Ahilya University, Indore 452017, India

Abstract

This study focused on the deleterious effect of anthracene (ANT) and role of a surfactant, Triton (TX-100), in recovery from inhibitory effect of ANT. Fast chlorophyll (Chl) fluorescence measurements were performed in wheat plants. Results revealed that maximum quantum yield of PSII, area over the fluorescence curve, performance index (PI), and reaction centre density was negatively affected by ANT treatment. The effects on PSII quantum efficiency, reaction centre density, absorption, and trapping were partially recovered by TX-100. PSII heterogeneity in terms of PSII antenna heterogeneity, corresponding to PSII α, β, and γ centres, and reducing side, corresponding to Q_B-reducing and Q_B-nonreducing centres, were also investigated. The damage caused by ANT to PSII antenna heterogeneity was recovered almost by 100% owing to TX-100.

Additional key words: anthracene; chlorophyll *a* fluorescence; photosystem II; heterogeneity; Triton X-100; wheat.

Introduction

Polycyclic aromatic hydrocarbons (PAHs) are chemical organic compounds that are composed of two or more fused aromatic rings. PAHs are generally formed by incomplete combustion of fossil fuels and other organic materials (Wheatly and Sadhra 2004). They are known to be carcinogenic to humans and other organisms (Kim *et al.* 2001). US Environmental Protection Agency (USEPA) has identified 16 PAHs including naphthalene, phenanthrene, and anthracene as priority pollutants, which form a subset of "toxic pollutants" (USEPA 2002). PAHs are under strong attention of the scientific community (Fazio and Howard 1983). These administrative regulations have encouraged scientists and engineers to identify the best remediation technologies from a variety of physical, chemical, and biological methods which can be used to remove these compounds from polluted sites.

Contamination of soils and ground water by toxic or hazardous pollutants is a widespread environmental problem and the removal of hydrophobic organic compounds (HOCs) from soils has become a major concern. PAH solubility in water is typically lesser than 10^{-4} M and PAHs are strongly absorbed in soils. Desorption from soils strongly limits an efficiency of remediation techniques.

In natural environment, plants are exposed to interaction of several exogenous factors. They have abilities to take in, transform, and accumulate many of the environmental pollutants including PAHs. It has been proved that PAHs influence biochemical and physiological processes in plants, similarly as other toxic organic compounds such as herbicides. They do not only change the processes of energetic metabolism, but also mechanisms associated with plant growth and development. In higher plants, the exposure to PAHs causes diminished biomass accumulation, chlorosis, and inhibition of photosynthesis (Huang *et al.* 1996, Oguntimehin *et al.* 2008). PAHs cause a decrease in photosynthetic pigment contents by a direct interaction with the pigment molecules or by inhibition of their synthesis (Kummerova *et al.* 2006, Oguntimehin *et*

Received 27 October 2016, *accepted* 19 January 2017, *published as online-first* 13 March 2017.
+Corresponding author; phone: +91-731-2477166; fax: +91-731-4263453, e-mail: anjanajajoo@hotmail.com
Abbreviations: ABS – absorption; ANT – anthracene; Chl – chlorophyll; CS – cross section; DCMU – 3-(3,4-dichlorophenyl)-1,1-dimethyl urea; DI_0 – dissipation; DM – dry mass; ET_0 – electron transport; F_0 – initial fluorescence; F_m – maximum fluorescence; FM – fresh mass; F_v – variable fluorescence; OEC – oxygen-evolving complex; OJ, JI, IP – phases of Chl *a* fluorescence induction curve; PAH – polycyclic aromatic hydrocarbons; *PEA* – plant efficiency analyser; PQ – plastoquinone; RC – reaction center; ROS – reactive oxygen species; TR_0 – trapping.
Acknowledgements: C. Sharma thanks Council of Science and Industrial Research (CSIR), India, for CSIR-Junior Research Fellowship (09/301(0126)/2014-EMRI). R.S. Tomar thanks Department of Science and Technology (DST), India for the Inspire Fellowship under Assured Opportunity for Research Careers (AORC) [IF-120412]. A. Jajoo thanks to Department of Science and Technology (DST), India for the Project (DST/RUS/RFBR/P-173). S. Mathur thanks University Grant Commission, (UGC), India for Post Doctoral Fellowship for Women (PDFWM-2014-15-GEMAD-23945).

al. 2010). Images from transmission electron microscopy have revealed that PAHs can cause gross deformation in chloroplasts and may lead to oxidation stress (Liu *et al.* 2009). PAHs have been found to enhance production of reactive oxygen species (ROS) in higher plants (Oguntimehin and Sakugawa 2009). Several studies have shown inhibitory effects of PAHs on donor and acceptor sides of PSII including oxygen evolving complex (OEC) and electron transport chain (Aksmann and Tukaj 2008, Kummerova *et al.* 2006). Over the last few decades, the effects of industrial activities has largely contributed to the presence of various harmful chemical substances in crops.

ANT (Fig. 1), together with other PAHs, is a persistent and toxic soil contaminant. ANT was found to inhibit the germination of seeds and the length of roots and shoots in seedlings of soybean (Tomar *et al.* 2015). Photosynthesis is the most important metabolic process in plants and its study provides information about the general ''health status'' of the plant. In order to assess the effects of ANT on photosynthesis (particularly PSII photochemistry), Chl *a* fluorescence has been measured. The measurement of Chl *a* fluorescence of plant is one of the most sensitive, noninvasive and quick method for the detection of compounds and environmental conditions which exhibit harmful effects on photosynthesis (Kalaji *et al.* 2016). Interestingly, the technique of Chl *a* fluorescence can be applied to a wide variety of samples including higher plants, algae, bacteria, lichens, diatoms, dinoflagellates, *etc*.

Among various approaches to analyse Chl *a* fluorescence signals, the so-called 'JIP-test', as pioneered by Strasser *et al.* (2004), is frequently employed in different areas of plant biology in order to understand the responses of photosynthetic apparatus to different physiological, genetic, and environmental conditions (Yusuf *et al.* 2010). This technique has been used very efficiently to detect PSII performance (Christen *et al.* 2007). The JIP-test is based on the theory of energy flow in thylakoid membranes (Force *et al.* 2003). Moreover, it provides relevant information about the probable fate of the absorbed energy, inflow and outflow of energy flux within PSII. Some of the parameters calculated using the JIP-test are related to energy fluxes for light absorption (ABS), trapping (TR) of excitation energy, and electron transport (ET) per reaction centre (RC) or per sample area called cross-section (CS). The polyphasic rise of fluorescence has been successfully employed in studies related to salt stress (Mehta *et al.* 2010), high-temperature stress (Mathur *et al.* 2011a), pH stress (Tongra *et al.* 2011), drought stress (Oukarroum *et al.* 2007), fluoranthene (Tomar and Jajoo 2013a), and chilling effect (Strauss *et al.* 2006).

Surfactants may be useful for the bioremediation of sites polluted with PAHs since they enhance the solubility of hydrophobic compounds (Boonchan *et al.* 1998). Many studies have been conducted to enhance the biodegradation of PAHs using surfactants in order to increase their solubility by decreasing the interfacial surface tension between PAHs and the soil/water interphase. When surfactant concentration is above the critical micelle concentration (CMC), micelle aggregates provide an additional hydrophobic area in the central region of micelles enhancing the aqueous solubility of PAHs (Li and Chen 2008). The addition of nonionic surfactants as additives has a positive effect on PAHs biodegradation (Grimberg *et al.* 1996, Volkering *et al.* 1995). However, some negligible (Ghosh *et al.* 1995) or even negative effects (Laha and Luthy 1992) have been reported. Thus, the application of surfactants in order to improve PAHs degradation may need to be optimized for a particular system and for a variety of factors influencing biodegradation, including surfactants type and concentration, PAH specificity, and the microorganisms present in the cultivation (Jin *et al.* 2007). Compared to ionic surfactants for the removal of PAHs, Perchloroethylene (PCE), and heavy metals in soils, TX-100 was more effective for remediation (Dianne *et al.* 2002, Zhu and Feng 2003).

Our work was divided in two parts. In the first part, effects of ANT on wheat growth, development, and photosynthetic parameters were studied, while in the second part, the effect of addition of Triton X-100 to ANT-treated soil was observed. The main goal of the present study was to study the effect of the presence of nonionic surfactant Triton X-100 on the degradation of low molecular mass PAH anthracene in wheat plants. Considerable attention was paid to the effect of this compound on the primary reactions of photosynthesis.

Materials and methods

Plant material: Wheat (*Triticum aestivum*, cv. Lok–1) was used in our experiment. Wheat seeds were allowed to germinate in 16 cm (length) plastic pots containing 700 g of soil with distilled water. Cultivation was done under PPFD of 300 μmol m^{-2} s^{-1} at 25°C. Ten seeds were sown in each pot. Plants were replenished every day in the way indicated in the text table below. Chl *a* fluorescence measurements were performed and subsequently photosynthetic parameters and PSII heterogeneity of experimental plants was determined.

Treatment	ANT	TX-100
CK	-	-
ANT	25 μM	-
TX-100	-	0.05%
ANT+TX-100	25 μM	0.05%

Solution preparation: Anthracene (ANT) (*Sigma Aldrich,* USA) was dissolved in acetone to make stock solution of 50 mM. Distilled water was added to it in order to prepare

an effective ANT concentration of 25 μM. It was found that the concentration of dissolvent did not affect seed germination and growth of seedlings and other physiological parameters, however, CK seeds were always exposed to the same concentration of acetone. *Triton X-100* (TX-100, *Himedia*, Mumbai, India) of 0.05% was prepared by dissolving in distilled water. For combined applications, 0.05% TX-100 and 25 μM ANT were dissolved in distilled water. Structure of ANT and TX-100 are shown in Fig. 1.

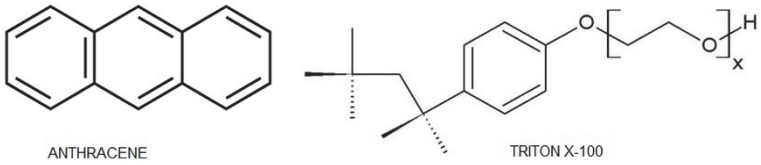

Fig. 1. Structure of anthracene and Triton X-100.

Chl *a* fluorescence induction kinetics was measured at room temperature using a plant efficiency analyzer (*PEA, Hansatech,* England). Excitation light of 650 nm (peak wavelength) from array of three light-emitting diodes was focused on the surface of the leaf to provide a homogenous illumination. Light intensity reaching the leaf was 3,000 μmol(photon) m^{-2} s^{-1} which was sufficient to generate maximal fluorescence (F_m) for all the treatments. The fluorescence signal was received by the sensor head during recording and was digitized in the control unit using a fast digital converter. Control leaves exhibited a polyphasic rise called O–J–I–P Chl *a* fluorescence transient; the O to J phase (ends at ~2 ms), the J to I phase (ends at ~30 ms) and I to P phase (ends at ~500 ms). The JIP test was named after the basic steps in the fluorescence transient, when plotted on a logarithmic time scale (Force *et al.* 2003). The measurements were performed 5 cm away from the tip and the bases, *i.e.*, in the middle portion on the ventral surface of the leaves, *i.e.*, the abaxial surface. Plants were dark-adapted for of 15 min before measurements. Details of parameters calculated from these curves have been put in the appendix. Performance index (PI) was calculated as:

$$PI_{[ABS]} = RC/ABS\ [\varphi_{P0}/(1-\varphi_{P0})\ \ \psi_0/(1-\psi_0)]$$

Antenna size heterogeneity: For determination of antenna heterogeneity, 3-(3,4-dichlorophenyl)-1,1-dimethyl urea (DCMU)-poisoning method was used (Hsu *et al.* 1989). The intact plant leaves were dipped into a beaker filled with 50 ml of DCMU solution (200 μM DCMU was dissolved in 1% ethanol) (Toth *et al.* 2005) for 2 h in dark. The leaves were then removed from the DCMU solution, wiped, and left in the air for ~30 min to avoid possible effects of anaerobiosis and then fluorescence measurements were recorded. Alpha (α), beta (β), and gamma (γ) centers were calculated from the complementary area growth curve. It involved the calculation of growth of the normalized complementary area, defined by the fluorescence induction curve and the line parallel with the maximum level of fluorescence (F_m) with time.

Heterogeneity of reducing side: Double hit (pulse) method was followed for the calculation of Q_B reducing and Q_B-nonreducing centers (Strasser *et al.* 2004). In this method two fluorescence transients were induced by two subsequent pulses [each of 1 s duration]. Q_B-reducing and Q_B-nonreducing centers were calculated as described in Mathur *et al.* (2011b).

Biomass: Three plants from each treatment (CK, ANT, TX-100, and ANT+TX-100) were harvested after 25 d of cultivation. Each plant was cut into small pieces and weighed for fresh biomass (FM). Same samples were then oven dried at 180°C for 4 h and then weighed for dry mass (DM).

Results and discussion

Growth parameters: The impact of ANT was studied on fresh and dry biomass (FM and DM) of wheat. Biomass production is regarded as a reliable external indicator of internal status of plant photosynthesis processes. When compared with CK, biomass production of FM and DM decreased by about 46% in the ANT-treated plants (Table 1). However, this inhibition was only 22% in ANT+TX-100 treatment. This showed that inhibitory effects of ANT were less pronounced in the presence of TX-100.

Chl *a* fluorescence induction kinetics was measured in order to evaluate the inhibitory effects of ANT and its recovery by TX-100 on photochemical efficiency of PSII in wheat plants. The Chl *a* induction curves (O-J-I-P) obtained after treatments revealed that the damage caused by ANT was partially recovered by TX-100 (Fig. 2). ANT caused a prominent change in the shape of fluorescence induction curve. F_0 increased significantly after the ANT treatment. This increase in F_0 could occurr due to many combined processes, such as functional disconnection of LHCII from the PSII complex or accumulation of inactive RCs (Yamane *et al.* 2000). The negative impact of F_0 was recovered almost to 100% by ANT+TX-100 treatment.

Table 1. Effect of 0.05% Triton X-100 (TX-100), 25 µM anthracene (ANT), 0.05% TX-100 + 25 µM ANT on different growth parameters in wheat plants. Each experiment was obtained from 4 replicates with 5 plants each. Values are given as mean ± standard deviation. CK – control plants.

Treatment	Fresh mass [%]	Dry mass [%]
CK	100 ± 1	100 ± 1
TX-100	74 ± 1*	94 ± 1*
ANT	54 ± 2*	67 ± 1*
TX-100+ANT	78 ± 1*	94 ± 1*

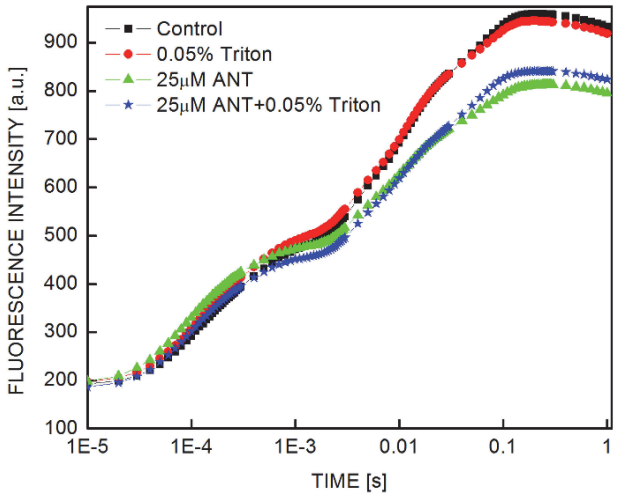

Fig. 2. Change in chlorophyll *a* fluorescence induction curves (OJIP) plotted on logarithmic scale in control, Triton X-100 (TX-100), 25 µM anthracene (ANT), 0.05% TX-100 + 25 µM ANT in wheat plants.

Chl *a* intensity decreased after the ANT treatment. ANT caused 15% decline in F_m as compared with CK. After the ANT+TX-100 treatment, the damage remained only 12% (Table 2) which means that TX-100 could recover the damage caused by ANT. Gradual decrease was observed in quantum yield of PSII after the ANT treatment which was evidenced by lower F_v/F_m. As compared with CK, quantum efficiency of PSII photochemistry declined by 8% in the ANT-treated plants; it remained only 4% lower in the plants with TX-100 (Table 2). Area represents an area over the fluorescence induction curve between F_0 and F_m and is proportional to the pool size of the electron acceptor Q_A on the reducing side of PSII and also Q_B, PQ and PSI acceptors (Strasser *et al.* 2004). Gradual drop approximately 24% in the area after the ANT treatment indicated that the electron transfer from RC to quinone pool was blocked (Table 2, Fig. 2). This blockage of quinone pool was partially restored in the ANT+TX-100-treated plants where only 16% decrease in the area was observed.

In order to find out the efficacy of ANT on wheat plants and effects of TX-100, PI was calculated. The photosynthetic PI is an indicator of sample vitality. It is the combined measurement of the RC/ABS, maximal energy flux that reaches the PSII RC and electron transport at the onset of illumination. $PI_{(ABS)}$ is a very sensitive index for stress and is used widely to compare the whole primary photochemical reactions (Chen and Cheng 2009), because it combines three main processes within PSII, (*1*) a component referring to the density of active PSII reaction centers per Chl (RC/ABS), (*2*) the component that describes the performance of the light reactions as $\Phi_{P0}/(1 - \Phi_{P0})$, and (*3*) the component that describes the performance of the dark redox reactions defined as $\psi_o/(1 - \psi_o)$. The performance index $PI_{(ABS)}$ is derived according to the principles of the Nernst equation for redox reactions (Christen *et al.* 2007). ANT caused a significant decrease in active PSII RCs followed by a decrease in size of the Chl antenna serving each RC and the reaction centre density (Table 3). Declined values of $\varphi_{P0}/(1 - \varphi_{P0})$ suggested that water-splitting complex of PSII and PSII photochemistry was affected due to the ANT treatment. A decrease in $\Psi_o/(1 - \Psi_o)$ indicated that the ANT treatment reduced vitality of the plants and caused damage and thus decreased the thermal dissipation of energy. This also means that ANT caused damage to PSII and decreased the conversion of excitation energy to electron transport. On the contrary, TX-100 caused recovery of all the three components of PI.

An alteration of PSII energy fluxes in response to ANT and its recovery by TX-100 was further visualized by energy pipeline models of photosynthetic apparatus. This is a dynamic model, where the energy fluxes in CK,

Table 2. Effect of 0.05% Triton X-100 (TX-100), 25 µM anthracene (ANT) on different Chl *a* transients in wheat plant. Each experiment consisted of four replicates with five plants each. Values are given as mean ± SD. CK – control plants. F_o – minimal fluorescence intensity at 50 µs; F_m – maximal fluorescence; F_v – variable fluorescence; F_v/F_m – ratio of variable to maximal fluorescence; Area – area above the curve up to F_m.

Treatment	F_0	F_m	F_v/F_m	Area
CK	188 ± 5 (100%)	960 ± 14 (100%)	0.80 ± 0.03 (100%)	12,304 ± 70 (100%)
TX-100	196 ± 8^{ns} (104%)	946 ± 11^{ns} (98%)	0.79 ± 0.02^{ns} (97%)	11,171 ± 65* (91%)
ANT	211 ± 4* (112%)	813 ± 6* (85%)	0.74 ± 0.06* (92%)	9,367 ± 56* (76%)
TX-100+ANT	191 ± 5^{ns} (101%)	841 ± 3* (89%)	0.77 ± 0.02^{ns} (96%)	10,256 ± 62* (84%)

Table 3. Effect of 25 μM anthracene (ANT) treatment and its recovery by Triton X-100 (TX-100) on components of performance index (PI) as derived from fluorescence induction kinetics shown in Fig. 2. CK – control plants. RC/ABS – density of reaction center per chlorophyll; φ_{Po} – maximum quantum yield of primary photochemistry; ψ_o – probability that a trapped exciton will move further than Q_A^-. All these three constitute performance index (PI).

Treatment	RC/ABS	$\varphi_{po}/(1-\varphi_{po})$	$\Psi_0/(1-\Psi_o)$
CK	0.753 ± 0.01 (100%)	4.10 ± 0.2 (100%)	1.48 ± 0.07 (100%)
TX-100	0.685 ± 0.03* (91%)	3.82 ± 0.15^{ns} (93%)	1.34 ± 0.02* (90%)
ANT	0.523 ± 0.02* (69%)	2.85 ± 0.3* (69%)	1.17 ± 0.06* (79%)
TX-100+ANT	0.613 ± 0.02* (81%)	3.4 ± 0.16* (83%)	1.35 ± 0.04* (91%)

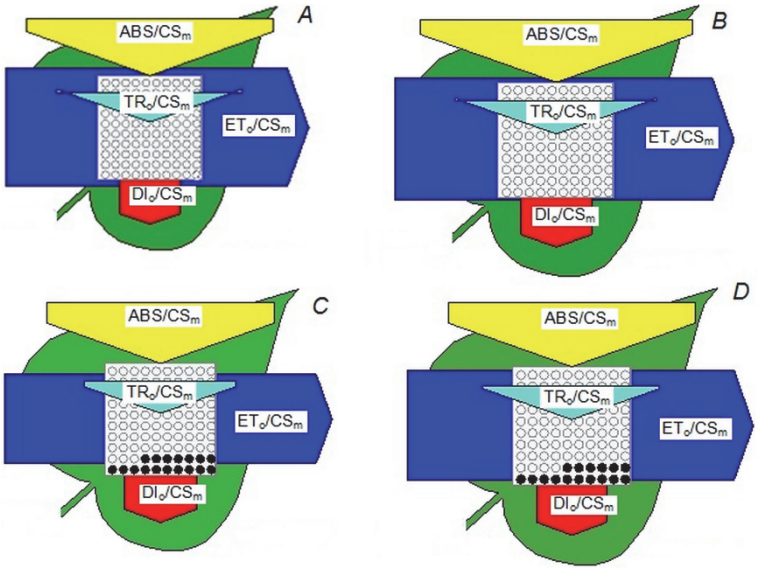

Fig. 3. Energy pipeline leaf model showing proportions of phenomenological energy flux parameters within a leaf, calculated per cross-section (CS_m) in control, 0.05% Triton X-100 (TX-100), 25 μM anthracene (ANT), and 25 μM ANT + 0.05% TX-100 in wheat plants. Width of the corresponding arrow denotes activity of that parameter. Empty and filled black circles indicate percentage of active and inactive reaction centres of PSII, respectively. *A* – Control; *B* – 0.05% TX-100; *C* – 25 μM ANT; *D* – 25μM ANT + 0.05% TX-100. ABS/CSm – absorption per CS; TRo/CSm – trapping at time zero per CS; DIo/CSm – dissipation at time zero per CS; ETo/CSm – electron transport at time zero per CS.

ANT-treated, and recovery by TX-100 were expressed by the width of corresponding arrows (Fig.3). The model also shows the changes in the active (open circles) and inactive (closed circles) PSII reaction centres per cross-section (RC/CS), as well as the flux of dissipated excitation energy at time zero (DI) (Fig.3).

The area of the arrows for various parameters, such as ABS/CS_m, TR/CS_m, ET/CS_m, and DI/CS_m, indicates the efficiency of light absorption, trapping and electron transport and dissipation per cross section of PS II, respectively (Tsimilli-Michael and Strasser 2008). It is that ANT caused a decline in ABS/CS_m, ET_0/CS_m, TR_0/CS_m. A decline in ABS/CS_m indicated a decrease of the energy absorbed per excited CS (Fig. 3). Electron transport decreased during the ANT treatment as compared with CK plants indicating lower energy absorption by antenna pigments (ABS/CS_m) and inactivation of reaction centre complexes. ANT acted on active reaction centres producing dissipative sinks for excitation energy. The ratio TR_0/CS_m gradually decreased with the ANT treatment indicating that trapping in reaction centres was affected significantly. A decrease in the density of active reaction centres (indicated as open circles) and an increase in the density of closed reaction centres (indicated as filled circles) was observed as a negative effect of ANT. An inactivation of PSII RCs resulted in a reduced trapping and thereby decreased ABS/CS_m (Fig. 3). The ratio DI/CS_m was not affected significantly by ANT indicating that energy was not dissipated in the form of heat, but was utilized in some other form. Partial recovery was observed with ANT+TX-100 treatment. TX-100 could recover the damage of ANT for electron transport, absorption per cross section and trapping, but inactive reaction centres were not recovered largely.

PSII heterogeneity: In contrast to other pigment protein complexes participating in photosynthetic light reaction, PSII shows diversity in its nature in functional and

Table 4. Changes in PSII heterogeneity in terms of antenna size heterogeneity (showing percentage of α, β, and γ PSII centres) and amount (in %) of Q_B-reducing and nonreducing centres in response to control (CK), 0.05% Triton X-100 (TX-100), 25 μM anthracene (ANT), 0.05% TX-100 + 25 μM ANT. Each experiment is a repeat of 4 replicates with 6 plants each. Values are given as mean ± standard deviation.

Treatment	α centers [%]	β centers [%]	γ centers [%]	Q_B reducing centers [%]	Q_B nonreducing centers [%]
Control	66 ± 1	28 ± 1	6 ± 1	79 ± 1	21 ± 1
TX-100	66 ± 2^{ns}	29 ± 1^{ns}	5 ± 2^{ns}	78 ± 1^{ns}	22 ± 2^{ns}
ANT	52 ± 2^{*}	42 ± 2^{*}	6 ± 2^{ns}	79 ± 2^{ns}	21 ± 1^{ns}
TX-100+ANT	62 ± 2^{ns}	34 ± 1^{ns}	4 ± 1^{ns}	79 ± 1^{ns}	21 ± 1^{ns}

structural aspects which is known as PSII heterogeneity. PSII has been found to undergo changes in its structural and functional heterogeneity in response to different abiotic stresses, such as salinity (Tomar *et al.* 2012), organic pollutants (Tomar and Jajoo 2015), high-temperature stress (Mathur *et al.* 2011b).

By using kinetic analysis of fluorescence induction curve for DCMU-poisoned chloroplasts (as described in Mathur *et al.* 2011b, Toth *et al.* 2005), PSII has been resolved into three components on the basis of antenna size, *i.e*., PSII α, PSII β, and PSII γ. This method provides direct information about the lifetime and the relative proportions of PSII α, PSII β, and PSII γ for ANT concentration and recovery by TX-100 in wheat plants. In case of antenna heterogeneity, ANT caused a change in the relative amount of α, β, and γ PSII centres (Table 4). The proportion (in %) of α, β, and γ PSII centres was found to be 66:28:6 in CK, 66:29:5 with TX-100, 52:42:6 with ANT, and 62:34:4 with ANT+TX-100. ANT converted active α into inactive β PSII centres, while γ centres remained unaffected. Alterations in α, β, and γ PSII centres are associated with downregulation of photochemical activity, damage of photosynthetic apparatus, and changes in the antenna organization**.** This conformational change was also supported by changes in the ratio of $\varphi_{po}/(1 - \varphi_{po})$ (Table 4). Concerning antenna heterogeneity, the number of inactive or less active β centres increased on account of the active α centres indicating that ANT caused alterations in the antenna of LHC of PSII. However, in the presence of TX-100, the inactive β centres were converted back to the active α centres (Table 4). This shows that TX-100 protected the plants from a deleterious effect of ANT and helped the plant to survive in PAH polluted soil.

A number of PSII centres, though photochemically competent, is unable to transfer electrons efficiently from electron acceptor Q_A^- to secondary electron acceptor Q_B. These centres are termed as Q_B-nonreducing centres. Heterogeneity of the reducing side was estimated by measuring relative amounts of Q_B-reducing and Q_B-nonreducing centres as described in Materials and methods. The population of Q_B-nonreducing centres was quantified, but no significant change was observed in the number of Q_B-nonreducing centres (Table 4) in response to ANT.

Conclusion: This work revealed severe phytotoxic effect of ANT on wheat as evident by a decrease in F_m, inactivation of active reaction centres, and suppressed PI. TX-100, a chemical surfactant, helped the plant to recover from severe effects of ANT. PSII heterogeneity is an important aspect of PSII which not only describes the PSII and LHC and antenna complexes, but also helps photosynthetic apparatus to cope and survive under various abiotic stresses. We showed that the damage caused or the changes in PSII heterogeneity, especially in PSII-antenna heterogeneity, due to ANT was largely recovered by TX-100. The PSII active centres, which were converted into inactive centres due to ANT, were again converted into their active status. This study proved that selection of a proper surfactant can be used to control the negative effect of PAH. We used the chemical surfactant, but in future, natural surfactants or bio-surfactants can be also tested in order to ameliorate the toxic effects of PAHs. To our knowledge, this is the first study which has emphasized on the use of fast Chl *a* fluorescence technique to investigate efficacy of appropriate remediation process for environmental pollutants.

References

Aksmann A., Tukaj Z.: Intact anthracene inhibits photosynthesis in algal cells: a fluorescence induction study on *Chlamydomonas reinhardtii* cw92 strain. – Chemosphere **74**: 26-32, 2008.

Boonchan S., Britz M.L., Stanley G.A.: Surfactant-enhanced biodegradation of high molecular weight polycyclic aromatic hydrocarbons by *Stenotrophomonas maltophilia*. – Biotechnol. Bioeng. **59**: 482-494, 1998.

Chen L.S., Cheng L.: Photosystem 2 is more tolerant to high temperature in apple (*Malus domestica* Borkh.) leaves than in fruit peel. – Photosynthetica **47**: 112-120, 2009.

Christen D., Schonmann S., Jermini M. *et al.*: Characterization and early detection of grapevine (*Vitis vinifera*) stress responses to esca disease by *in situ* chlorophyll fluorescence and comparison with drought stress. – Environ. Exp. Bot. **60**: 504-514, 2007.

Dianne J., Luning P., Parmely H.: Solubilization of polycyclic aromatic hydrocarbon mixtures in micellar non-ionic surfactant solutions. – Water Res. **36**: 3463, 2002.

Force L., Critchley C., Van Rensen J.J.S.: New fluorescence parameters for monitoring photosynthesis in plants. – Photosynth. Res. **78**: 17-33, 2003.

Grimberg S.J., Stringfellow W.T., Aitken M.D.: Quantifying the biodegradation of phenanthrene by *Pseudomonas stutzeri* P16 in the presence of a nonionic surfactant. – Appl. Environ. Microbiol. **62**: 2387-2392, 1996.

Hsu B.D., Lee Y.S., Jang Y.R.: A method for analysis of fluorescence induction curve from DCMU-poisoned chloroplasts. – Biochim. Biophys. Acta **975**: 44-49, 1989.

Huang X.D., Zeiler L.F., Dixon D.G. *et al.*: Photoinduced toxicity of PAHs to the foliar regions of *Brassica napus* (Canola) and *Cucumbis sativus* (Cucumber) in simulated solar radiation. – Ecotoxicol. Environ. Safe. **35**: 191-197, 1996.

Jin D., Jiang X., Jing X. *et al.*: Effect of concentration, head group, and structure of surfactants on the degradation of phenanthrene. – J. Hazard. Mater. **144**: 215-221, 2007.

Kalaji H.M., Jajoo A., Oukarroum A. *et al.*: Chlorophyll *a* fluorescence as a tool to monitor physiological status of plants under abiotic stress conditions. – Acta Physiol. Plant. **38**: 102-112, 2016.

Kim I.S., Park J.S., Kim K.W.: Enhanced biodegradation of polycyclic aromatic hydrocarbons using non-ionic surfactants in soil slurry. – Appl. Geochem. **16**: 1419-1428, 2001.

Kummerová M., Barták M., Dubová J. *et al.*: Inhibitory effect of fluoranthene on photosynthetic processes in lichens detected by chlorophyll fluorescence. – Ecotoxicology **15**: 121-131, 2006.

Laha S., Luthy R.G.: Effects of nonionic surfactants on the solubilization and mineralization of phenanthrene in soil-water systems. – Biotechnol. Bioeng. **40**: 1367-1380, 1992.

Li J.L., Chen B.H.: Effect of non-ionic surfactants on biodegradation of phenanthrene by a marine bacteria of *Neptunomonas naphathovarans*. – J. Hazard. Mater. **162**: 66-73, 2009.

Liu H., Weisman D., Ye Y.B. *et al.*: An oxidative stress response to polycyclic aromatic hydrocarbon exposure is rapid and complex in *Arabidopsis thaliana*. – Plant Sci. **176**: 357-382, 2009.

Mathur S., Jajoo A., Mehta P. *et al.*: Analysis of elevated temperature induced inhibition of Photosystem II using chlorophyll *a* fluorescence induction kinetics in wheat leaves. – Plant Biol. **13**: 1-6, 2011a.

Mathur S., Allakhverdiev S.I., Jajoo A.: Analysis of the temperature stress on the dynamic of antenna size and reducing side heterogeneity of photosystem II in wheat leaves (*Triticum aestivum*). – BBA-Bioenergetics **1807**: 22-29, 2011b.

Mehta P., Jajoo A., Mathur S. *et al.*: Chlorophyll *a* fluorescence study revealing effects of high salt stress on photosystem II in wheat leaves. – Plant Physiol. Bioch. **48**: 16-20, 2010.

Oguntimehin I., Eissa F., Sakugawa H.: Negative effects of fluoranthene on the ecophysiology of tomato plants (*Lycopersicon esculentum Mill*) fluoranthene mists negatively affected tomato plants. – Chemosphere **78**: 877-884, 2010.

Oguntimehin I., Sakugawa H.: Interactive effects of simultaneous ozone and fluoranthene fumigation on the eco-physiological status of the evergreen conifer, Japanese red pine (*Pinus densiflora* Sieb et Zucc.). – Ecotoxicology **18**: 100-109, 2009.

Oguntimehin I., Nakatani N., Sakugawa H.: Phytotoxicities of fluoranthene and phenanthrene deposited on needle surfaces of the evergreen conifer, Japanese red pine (*Pinus densiflora* Sieb. et Zucc.). – Environ. Pollut. **154**: 264-271, 2008.

Oukarroum A., El Madidi, S.E., Schansker G. *et al.*: Probing the responses of barley cultivars (*Hordeum vulgare* L.) by chlorophyll *a* fluorescence OLKJIP under drought stress and re-watering. – Environ. Exp. Bot. **60**: 438-446, 2007.

Prak D.J.L., Pritchard P.H.: Solubilization of polycyclic aromatic hydrocarbon mixtures in micellar non-ionic surfactant solutions. – Water Res. **36**: 3463-3472, 2002.

Strasser R.J., Tsimilli-Michael M., Srivastava A.: Analysis of the chlorophyll *a* fluorescence transient. – In: Papageorgiou G.C. (ed): Chlorophyll *a* Fluorescence: A Signature of Photosynthesis, Advances in Photosynthesis and Respiration. Pp. 321-362. Springer, Dordrecht 2004.

Strauss A.J., Krüger G.H.J., Strasser R.J. *et al.*: Ranking of dark chilling tolerance in soybean genotypes probed by the chlorophyll *a* fluorescence transient O-J-I-P. – Environ. Exp. Bot. **56**: 147-157, 2006.

Tomar R.S., Sharma A., Jajoo A.: Assessment of phytotoxicity of anthracene in soybean (*Glycine max.*) with a quick method of chlorophyll fluorescence. – Plant Biol. **17**: 870-876, 2015.

Tomar R.S., Jajoo A.: Photomodified fluoranthene exerts more harmful effects as compared to intact fluoranthene by inhibiting growth and photosynthetic processes. – Ecotox. Environ. Safe. **122**: 31-36, 2015.

Tomar R.S., Jajoo A.: A quick investigation of the detrimental effects of environmental pollutant polycyclic aromatic hydrocarbon fluoranthene on the photosynthetic efficiency of wheat (*Triticum aestivum*). – Ecotoxicology **22**: 1313-1318, 2013a.

Tomar R.S., Jajoo A.: Alteration in PSII heterogeneity under the influence of polycyclic aromatic hydrocarbon (fluoranthene) in wheat leaves (*Triticum aestivum*). – Plant Sci. **209**: 58-63, 2013b.

Tomar R.S., Mathur S., Allakhverdiev S.I. *et al.*: Changes in PS II heterogeneity in response to osmotic and ionic stress in wheat leaves (*Triticum aestivum*). – J. Bioenerg. Biomembr. **44**: 411-419, 2012.

Tongra T., Mehta P., Mathur S. *et al.*: Computational analysis of fluorescence induction curves in intact spinach leaves treated at different pH. – Biosystems **103**: 158-163, 2011.

Toth S.Z, Schansker G., Strasser R.J.: In intact leaves, the maximum fluorescence level (F_m) is independent of the redox state of the plastoquinone pool: a DCMU-inhibition study. – BBA-Bioenergetics **1708**: 275-282, 2005.

Tsimilli-Michael M., Strasser R.J.: *In vivo* assessment of stress impact on plants vitality: Applications in detecting and evaluating the beneficial role of mycorrization on host plants. – In: Varma A. (ed.): Mycorriza. Pp. 679-703, Springer Verlag, Berlin, Heidelberg 2008.

USEPA (Environmental Protection Agency) Procedures for the Derivation of Equilibrium Partitioning Sediment Benchmarks (ESBs) for the Protection of Benthic Organisms: PAH Mixtures. EPA-600-R-02-013. Office of Research and Development, Washington, DC, 20460 (draft), 2002.

Volkering F., Breure A.M., van Andel J.G. *et al.*: Influence of nonionic surfactants on bioavailability and biodegradation of polycyclic aromatic hydrocarbons. – Appl. Environ. Microbiol. **61**: 1699-1705, 1995.

Wheatley A.D., Sadhra S.: Polycyclic aromatic hydrocarbons in solid residues from waste incineration. – Chemosphere **55**: 743-749, 2004.

Yamane Y., Shikanai T., Kashino Y. *et al.*: Reduction of Q_A in the dark: another cause of fluorescence F_o increases by high temperature in higher plants. – Photosynth. Res. **63**: 23-34, 2000.

Yusuf M.A., Kumar D., Rajwanshi R. *et al.*: Overexpression of gamma-tocopherol methyl transferase gene in transgenic *Brassica juncea* plants alleviates abiotic stress: physiological and chlorophyll fluorescence measurements. – Biochim. Biophys. Acta **1797**: 1428-1438, 2010.

Zhu L., Feng S.: Synergistic solubilization of polycyclic aromatic hydrocarbons by mixed anionic-nonionic surfactants. – Chemosphere **53**: 459-467, 2003.

Appendix

Description	Fluorescence parameters
Technical parameters	
Fluorescence intensity at 50 μs, minimal Fluorescence F_o	O
Fluorescence intensity at 2 ms	J
Fluorescence intensity at 30 ms	I
F_m, maximal fluorescence intensity	P
Maximal variable fluorescence, $[F_m - F_{50\,\mu s}]$	F_v
Area between the fluorescence curve and F_m	Area
The density of reaction centres per chlorophyll	$RC/ABS = (RC/TR_o)\ (TR_o/ABS)$
The phenomenological fluxes expressed per cross section of the leaf tissue [CS]	
Absorption per CS	ABS/CS_m approximated by F_m
Trapping at time zero per CS	$TR_o/CS_m = [TR_o/ABS]/[ABS/CS]$
Dissipation at time zero per CS	$DI_o/CS_m = [ABS/CS]-[TR_o/CS]$
Electron transport at time zero per CS	$ET_o/CS_m = [ET_o/RC][RC/CS]$
The yields [flux ratios]	
Maximum quantum yield of primary photochemistry	$\varphi_{Po} = TR_o/ABS = [F_m - F_o]/F_m = F_v/F_m$
Probability that a trapped exciton moves an electron further than Q_A^-	$\psi_o = ET_o/TR_o = 1-V_j$
Performance index	$PI_{ABS} = RC/ABS\ [\varphi_{P0}/(1-\varphi_{P0}).\psi_0/(1-\psi_0)]$